

Article

Inhibition of Fungal Growth and Aflatoxin B₁ Synthesis in *Aspergillus flavus* by Plasma-Activated Water

Qihuan Yao ^{1,2,3,†}, Hangbo Xu ^{1,2,3,†}, Jie Zhuang ⁴ , Dongjie Cui ^{2,*}, Ruonan Ma ^{1,3,*} and Zhen Jiao ^{1,2,3}

¹ Zhengzhou Research Base, State Key Laboratory of Cotton Biology, School of Agricultural Sciences, Zhengzhou University, Zhengzhou 450001, China; jiaozhen@zzu.edu.cn (Z.J.)

² Henan Key Laboratory of Ion-Beam Bioengineering, School of Agricultural Sciences, Zhengzhou University, Zhengzhou 450052, China

³ Sanya Institute, Zhengzhou University, Zhengzhou 450001, China

⁴ Suzhou Institute of Biomedical Engineering and Technology, Chinese Academy of Sciences, Suzhou 215163, China

* Correspondence: cuidongjie0323@zzu.edu.cn (D.C.); maruonan@zzu.edu.cn (R.M.)

† These authors contributed equally to this work.

Abstract: The gaseous reactive oxygen/nitrogen species (RONS) generated by cold atmospheric plasma (CAP) can effectively inactivate *Aspergillus flavus* (*A. flavus*) and prolong the shelf-life of food. Plasma-activated water (PAW) is the extension of cold plasma sterilization technology. Without the limitation of a plasma device, PAW can be applied to more scenarios of food decontamination. However, the efficacy of PAW as a carrier of RONS for eradicating *A. flavus* or inhibiting its growth remains unclear. In this study, the immediate fungicidal effect and long-term inhibitory effect of PAW on *A. flavus* were investigated. The results demonstrated that 60-min instant-prepared PAW could achieve a 3.22 log reduction CFU/mL of *A. flavus* and the fungicidal efficacy of PAW gradually declined with the extension of storage time. Peroxynitrite (ONOO⁻/ONOOH) played a crucial role in this inactivation process, which could damage the cell wall and membrane structure, disrupt intracellular redox homeostasis, and impair mitochondrial function, ultimately leading to fungal inactivation. In addition to the fungicidal effect, PAW also exhibited fungistatic properties and inhibited the synthesis of aflatoxin B₁ (AFB₁) in *A. flavus*. By analyzing the cellular antioxidant capacity, energy metabolism, and key gene expression in the AFB₁ synthesis pathway, it was discovered that PAW can significantly reduce ATP levels, while increasing SOD and CAT activity during 5-d cultivation. Meanwhile, PAW effectively suppressed the expression of genes related to AFB₁ synthesis.

Keywords: plasma-activated water; *Aspergillus flavus*; peroxynitrite; fungicidal effect; inhibitory effect



Citation: Yao, Q.; Xu, H.; Zhuang, J.; Cui, D.; Ma, R.; Jiao, Z. Inhibition of Fungal Growth and Aflatoxin B₁ Synthesis in *Aspergillus flavus* by Plasma-Activated Water. *Foods* **2023**, *12*, 2490. <https://doi.org/10.3390/foods12132490>

Academic Editor: Lara Manyes

Received: 30 April 2023

Revised: 20 June 2023

Accepted: 21 June 2023

Published: 26 June 2023



Copyright: © 2023 by the authors. Licensee MDPI, Basel, Switzerland. This article is an open access article distributed under the terms and conditions of the Creative Commons Attribution (CC BY) license (<https://creativecommons.org/licenses/by/4.0/>).

1. Introduction

Aspergillus flavus (*A. flavus*) is a soil-borne saprophytic fungus that infects and contaminates crops [1]. *A. flavus* produces aflatoxins, which are highly toxic and pose serious threats to food quality, safety, and human health [2]. It has been reported that about 25% of global food crops worldwide are contaminated with aflatoxins [3]. Therefore, the decontamination of *A. flavus* and aflatoxins are critical issues that need to be addressed [4].

Cold atmospheric plasma (CAP) attracts increasing attention as a novel non-thermal technology for food decontamination and preservation [5]. CAP is generated by electrical discharge, which refers to ionized gas that processes a variety of reactive oxygen/nitrogen species (RONS). These RONS have been proven to be the major agents in microbial inactivation [6,7]. Numerous investigations have also confirmed the antifungal effects of CAP against *A. flavus*. For instance, Dasan et al. demonstrated that CAP could compromise the integrity of *A. flavus* spore cells by scanning electron microscopy (SEM) observations [8,9]. The decontamination efficacy was found to increase with the increasing applied reference voltage and frequency. Upon further study, Dasan et al. discovered that air plasma was

more effective than nitrogen plasma in eliminating *A. flavus* spores due to the formation of ROS in the presence of oxygen [10]. Devi et al. found that a 60-W and 15-min CAP treatment could effectively inactivate 99.5% of *A. flavus*, and significantly reduce the production of AFB₁ by 96.8% [11]. Mošovská and Ott et al. employed optical emission and absorption spectroscopy to confirm the production of gaseous RONS, e.g., hydroxyl radical ($\cdot\text{OH}$), ozone (O_3), nitrogen oxides (NO_x). These RONS induce the inactivation of *A. flavus* [2,12]. Recently, Lin et al. employed a novel rotary plasma jet to inhibit *A. flavus* and found CAP effectively inhibited the growth of *A. flavus* on peanuts. Moreover, the content of AFB₁ was significantly reduced. Aflatoxin concentrations in CAP treated (200 W and 5 min) and untreated peanuts were 16.5 and 363.7 ppb after 29-d storage, respectively [3].

These aforementioned research articles demonstrated the decontamination ability of CAP against *A. flavus* and Aflatoxin. However, CAP decontamination faces plenty of problems in practical application. For example, the samples with irregular shapes cannot be treated homogeneously by CAP [13] and the large-scale processing is difficult to achieve [14]. Moreover, the UV and electromagnetic fields in CAP may pose potential hazards to the operators and damage delicate biological materials [15]. Thus, to successfully transfer CAP decontamination into the practical application, a novel CAP-based technology should be proposed. Recently, plasma-activated water (PAW) has been born to meet the need. PAW is generated by CAP treatment of water, which also possesses rich RONS (such as $\cdot\text{OH}$, superoxide anion ($\cdot\text{O}_2^-$), singlet oxygen ($^1\text{O}_2$), hydrogen peroxide (H_2O_2), nitrate (NO_3^-), nitrite (NO_2^-), and peroxynitrite ($\text{ONOO}^-/\text{ONOOH}$)) and can inactivate various microorganisms (such as viruses, bacteria, and fungi) [16–22]. Without the limitation of the CAP device, PAW can be used as a carrier of RONS to decontaminate foods in a variety of scenarios [23]. However, the decontamination effects of PAW against *A. flavus* and Aflatoxin are not clear yet.

Herein, this study investigated the immediate fungicidal effect and long-term inhibitory effect of PAW on *A. flavus*. A novel plasma jet device was employed to prepare PAW, and the electrochemical properties (oxidation-reduction potential (ORP), pH, and electrical conductivity) of PAW were detected. Meanwhile, the concentration of ONOO^- and NO_3^- in PAW was also measured. Furthermore, the inactivation efficiency of PAW against *A. flavus* at different storage times and its relationship with ONOO^- concentration were analyzed. Then, the possible inactivation mechanism of PAW against *A. flavus* was analyzed by measuring the cell membrane integrity, intracellular RONS, and mitochondrial membrane potential. In addition to the inactivation effect, the inhibition effect of PAW on AFB₁ synthesis was also investigated via the analysis of the changes in antioxidant capacity, energy metabolism, and the expression of key genes in the aflatoxin synthesis pathway of *A. flavus*.

2. Experimental Setup and Methods

2.1. The Preparation of PAW

A novel CAP jet device was employed to treat the water for the preparation of PAW (Figure 1a). The plasma jet device was comprised of an HV copper electrode in the chamber and the outer copper electrode as the ground electrode. The electrodes were separated by a ceramic tube and were driven by the high-voltage power supply (Suodifu, Zhengzhou, China). Air was used as the carrier gas with a flow rate of 10 L/min, and the length of the jet plume was about 30 mm. The discharge voltage was measured by a high-voltage probe (Tektronix, P6015A), and the discharge current was measured by the current probe (Pearson Electronics, 2877). The data of the waveforms were recorded by an oscilloscope (Teledyne, WaveSurfer 3000). As shown in Figure 1b, the discharge frequency was 33 kHz and the voltage had a peak-to-peak value of 8 kV. The power was sustained at approximately 240 W. 50 mL sterile distilled water was treated by CAP for 2 min to acquire the PAW solution. After being stored for different times, PAW was utilized to treat *A. flavus*.

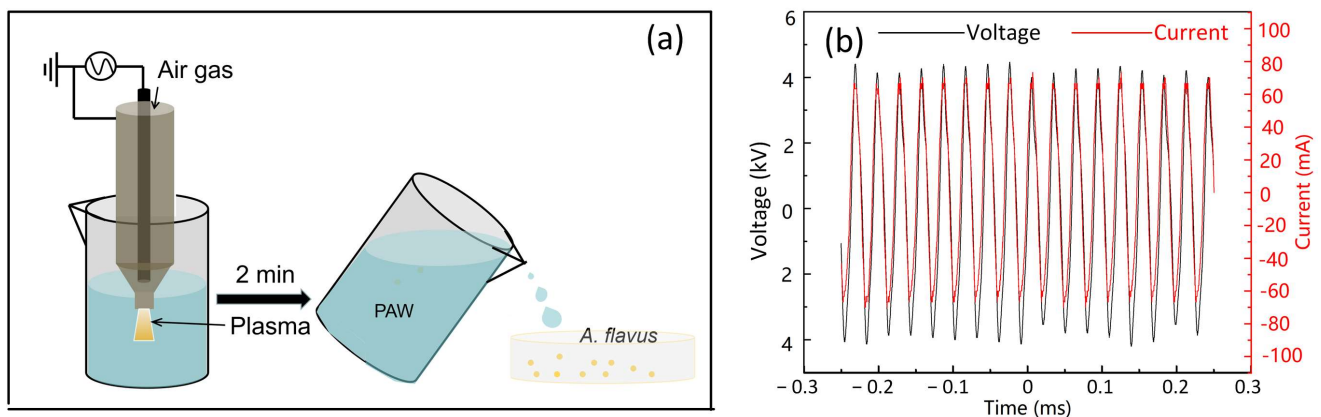


Figure 1. (a) Schematic diagram of CAP jet device, PAW preparation, and PAW treatment of *A. flavus*. (b) Current and voltage waveforms of CAP jet.

2.2. Measurements of Optical Emission Spectra

During the processing of CAP discharge, optical emission spectra (OES) were detected by AvaSpec-ULS 4096CL-EVO (Avantes, Lafayette, CO, USA). The probe of fiber optics cable was used to acquire the light signals at a distance approximately 5 mm away from the end of the plasma jet plume.

2.3. Measurements of pH, ORP, Electrical Conductivity, and ONOO⁻ in PAW

The pH and ORP of PAW were measured after storage at different times by the multimeter pH and Redox (Mettler-Toledo, Zurich, Switzerland). The electrical conductivity of PAW was measured after storage at different times by an electric conductivity meter. The ONOO⁻ concentration in PAW was measured after storage for different times by the method provided by Tarabová et al. [24]. The probe of 2, 7-dichlorodihydrofluorescein diacetate (H₂DCFDA) was used for ONOO⁻ detection. NO₃⁻ concentration in PAW was measured after storage for different times by spectrophotometric method [25].

2.4. The Culture of *A. flavus* Spores and Mycelium

A. flavus spores were harvested in 20 mL of sterile deionized water from 7-day-old cultures grown on potato dextrose agar (PDA) at 30 °C. After filtration with the sterile gauze, centrifuged, and washed with the sterile deionized water, the concentration of *A. flavus* spores was adjusted to about 7 log CFU/mL for PAW treatment. In addition, *A. flavus* spores were inoculated on PDA and cultivated for two days at 30 °C. Then, the mycelium was collected and treated by PAW.

2.5. Detection of *A. flavus* Inactivation Efficiency

The inactivation efficiency of *A. flavus* by PAW was evaluated by colony forming units (CFU). *A. flavus* spores were treated by PAW after storage at different times, and then centrifuged at 8000 × *g* for 5 min and resuspended by the sterile deionized water. A 10-fold serial dilution of 100 μL of spore suspensions were spread on PDA. Then the plates were placed in the incubator for the spore growth at 30 °C. After 48 h cultivation, the CFU was counted.

2.6. Detection of Cell Membrane Integrity, Intracellular RNS and Mitochondrial Membrane Potential

After treatment with the instant-prepared PAW, the cell membrane integrity, intracellular RNS, and mitochondrial membrane potential of *A. flavus* were measured by flow cytometry and fluorescence microscope. Propidium iodide (PI) was used to detect the cell membrane permeability. 2', 7'-dichlorofluorescein diacetate (H₂DCF-DA), 3-Amino,4-aminomethyl-2',7'-fluorescein, and diacetate (DAF-FM DA) were used to detect the in-

tracellular ONOO⁻ and NO. 5,5',6,6'-tetrachloro-1,10,3,3'-tetraethylimidacarbocyanine iodide (JC-1) (Beyotime, Shanghai, China) was used to detect the mitochondrial membrane potential (MMP). After PAW treatment, *A. flavus* spores or mycelium were centrifuged and resuspended by phosphate-buffered saline (PBS), and their probes were added into the suspensions and incubated at 30 °C for 30 min in the dark. Then, *A. flavus* spores or mycelium were washed by PBS, and the mean fluorescence intensity (MFI) of *A. flavus* spores was analyzed by flow cytometry. The fluorescence intensity of mycelium was observed by fluorescence microscope.

2.7. Determination of AFB₁ Concentration

AFB₁ was detected with enzyme-linked immunosorbent assay (ELISA). After treatment with the instant-prepared PAW, *A. flavus* was inoculated onto PDA and cultivated for 2, 3, and 5 d. The AFB₁ concentrations of *A. flavus* at different culture times were analyzed by the AFB₁ ELISA Kit (Finderbio, Shenzhen, China). The kit consisted of a 96-well microtiter plate pre-coated with conjugate antigen, horseradish enzyme marker, antibody, standard of AFB₁, and other supporting reagents. AFB₁ in the samples can compete with conjugate antigen pre-coated in the plate, and inhibit AFB₁ antibodies. TMB (3,3',5,5'-tetramethylbenzidine) was used for color development. The absorbance value of the sample was negatively correlated with the content of AFB₁. The amount of AFB₁ in the samples can be calculated by comparing it with the standard curve. The detection limit of this ELISA kit was 1 ppb.

2.8. Determination of SOD Activity, CAT Activity, and ATP Content

After treatment with the instant-prepared PAW, *A. flavus* was inoculated onto PDA and cultivated for 2, 3, and 5 d. The SOD activity, CAT activity, and ATP content of *A. flavus* at different culture times were measured. Mycelia were freeze-dried in liquid nitrogen and grounded. After that, the samples were homogenized in PBS and centrifuged in 7000 × *g* for 15 min at 4 °C. The supernatant was used for the detection of ATP content, total protein concentration, and enzyme activity. The ATP level was measured with a bioluminescence assay kit (Beyotime, Shanghai, China). The total protein concentration of *A. flavus* was determined by Bradford assay (Protein standard: bovine serum albumin). SOD and CAT activities were detected by commercial kits (Cu/Zn-SOD and Mn-SOD Assay Kit, Catalase Assay Kit, Beyotime, Shanghai, China). The SOD or CAT activities were expressed as the SOD activity or CAT activity divided by total protein concentration.

2.9. Detection of the Gene Expression Level

After treatment with the instant-prepared PAW, *A. flavus* was inoculated onto PDA and cultivated for 2, 3, and 5 days for the extraction of RNA. The cultures were harvested and homogenized in liquid nitrogen. Total RNA was extracted with TRIzol Reagent (ThermoFisher Scientific, Carlsbad, USA) and transcribed to cDNA by the *Evo M-MLV* RT premix Kit (Accurate Biology, Changsha, China) according to the manufacturer's protocol. The relative expression of aflatoxin biosynthesis genes (*aflD*, *aflP*, *aflQ*, *aflR*, *aflS*) was determined by real-time fluorescence quantitative PCR (RT-qPCR). The primers for the amplification of these 5 genes and a reference gene (β -tubulin) were reported by the literature [26]. The sequences and amplification efficiency of each pair of primers were also shown in the Supporting Information (Table S1 and Figure S1). The PCR reaction contained cDNA as a template, gene-specific primers, and 2 × SYBR[®] Green *Pro Taq* HS Premix (Accurate Biology, Changsha, China). qPCR was carried out at 95 °C for 2 min; 40 cycles of 95 °C for 15 s, 58 °C for 15 s, and 68 °C for 20 s (Roche's automatic fluorescence PCR analyzer (LightCycler480)); melting curves were performed according to the default parameters of the instrument. The 2^{- $\Delta\Delta$ Ct} values were obtained using the β -tubulin gene as an internal reference [27].

2.10. Statistical Analysis

Three replicate experiments were carried out to obtain the data. Values were expressed as the mean value \pm standard deviation (SD). Analysis of variance (ANOVA) in SPSS statistical package 22.0 (SPSS statistical package 22.0, New York, NY, USA) was used to perform the statistical analysis. Student–Newman–Keuls multiple range test was employed to identify the significant differences between samples with a confidence level at $p < 0.05$.

3. Results and Discussion

3.1. The OES of Plasma Jet

To identify the major excited reactive species, OES in the wavelength of 200–1000 nm were observed. As was shown in Figure 2, the second positive system N_2 ($C^3\Pi_u \rightarrow B^3\Pi_g$) emissions (313, 337, 357, and 380 nm), NO_γ (200–300 nm), O (777 and 844 nm) and $\cdot OH$ band (309 nm) could be identified [28]. The electron impact dissociation of O_2 molecules led to the formation of O (Equation (1)). Simultaneously, the band in N_2 molecules can also be broken by vibrational excitation and dissociation (Equation (2)) [29]. The excited N_2 molecules can dissociate H_2O molecules to form $\cdot OH$ (Equations (3) and (4)). Nitrogen oxides can be formed from the reactions of the dissociated N_2 and O_2 (Equations (5) and (6)) [7]. These gas-phase RONS can further react with water molecules to produce various secondary RONS in liquids [17].

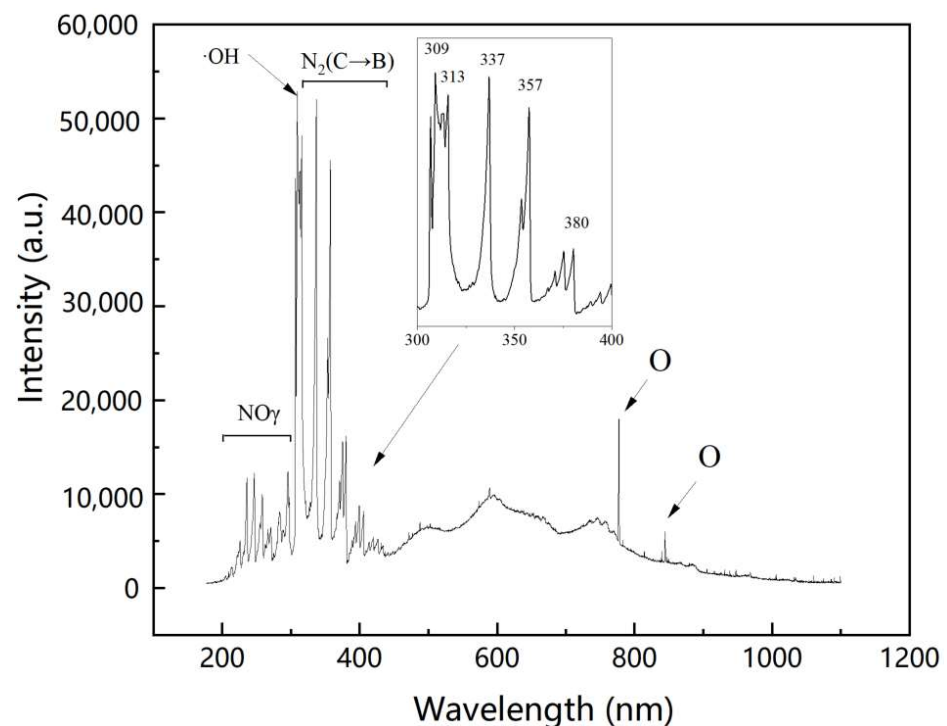


Figure 2. OES of the plasma in the range of 200–1100 nm.

3.2. Physicochemical Properties of PAW

The plasma gas-liquid interaction can change the physicochemical properties of the liquid. ORP can reflect the total oxidation level of the solution. Generally speaking, the higher ORP, the stronger oxidation of the solution. It has been reported that the ORP of water after CAP treatment was increased [20]. Compared to water (~230 mV), the ORP of PAW was increased to about 560 mV (Figure 3a). In addition to ORP, the acidification of water is another property after CAP treatment. As was shown in Figure 3b, the pH value of PAW was about 2.8. The results of OES demonstrated the generation of nitrogen oxides. The dissolution of nitrogen oxides in the liquid can form NO_2^- , NO_3^- , and H^+ ions, thus leading to a drop in pH (Equations (7) and (8)) [7]. Electrical conductivity was also measured. As was shown in Figure 3c, the electrical conductivity of PAW was increased to about 400 $\mu\text{S}/\text{cm}$, indicating that a number of ions existed in PAW. These ions, especially RONS, play important roles in fungal inactivation.

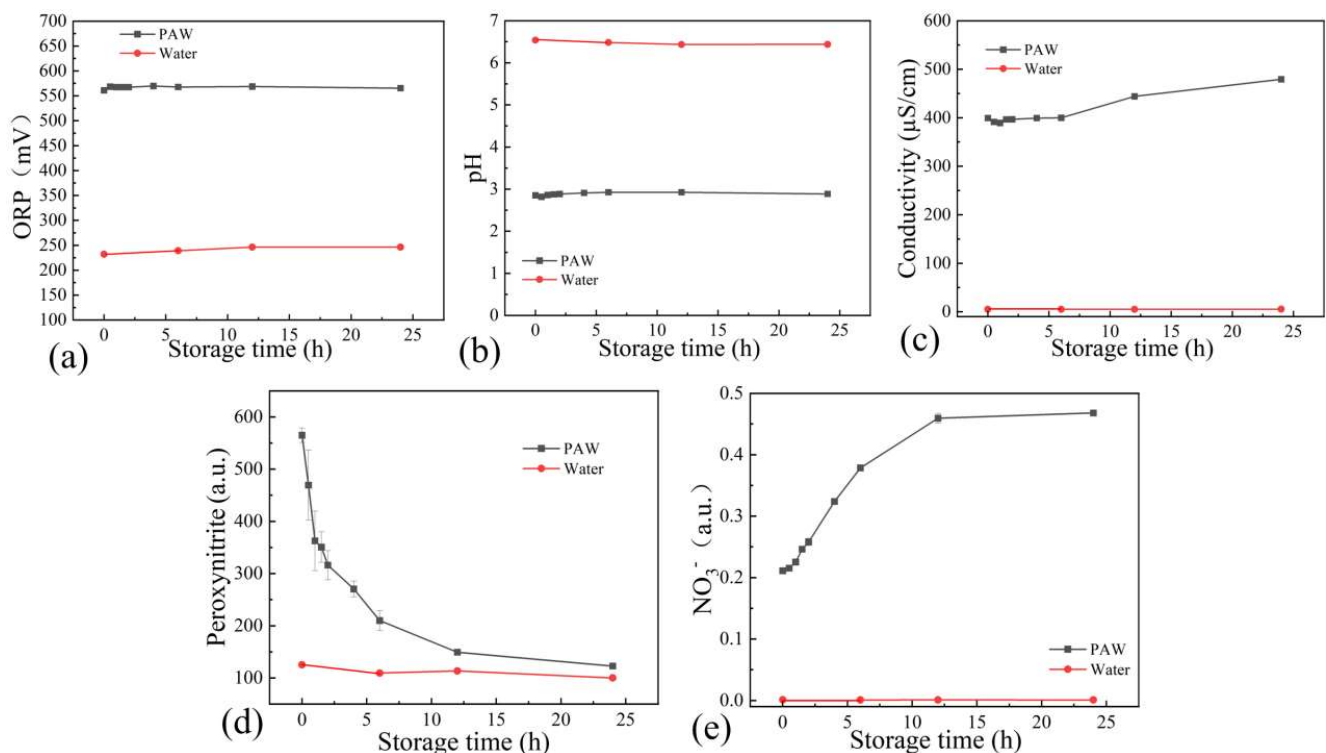
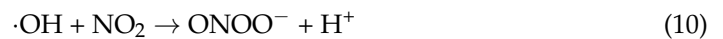
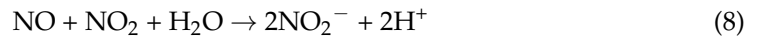
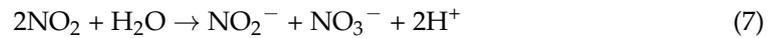


Figure 3. The changes of (a) ORP, (b) pH, (c) electrical conductivity, (d) ONOO^- , and (e) NO_3^- in PAW within 24-h storage.

Peroxynitrite was reported to be the critical RONS in PAW, which was a strong oxidant agent including both anionic (ONOO^-) and protonated (ONOOH) forms [16]. Peroxynitrite can be generated in PAW through many pathways. Firstly, $\cdot\text{O}_2^-$ reacted with NO , and $\cdot\text{OH}$ reacted with NO_2 to form ONOO^- (Equations (9) and (10)) [30]. Secondly, ONOO^- can be formed by the dissolution of gaseous N_2O_5 from the plasma region (Equation (11)). In addition, ONOO^- can be formed via the reaction of NO_2^- and H_2O_2 (Equation (12)) [31]. Peroxynitrite was a kind of short-lived RONS. As was shown in Figure 3d, ONOO^- was gradually decreased with the increasing storage time. Given that ONOOH would be the dominant form when the pH was lower than 6.8 ($\text{p}K_a$ of ONOOH), ONOOH was the dominant form in PAW, whose pH was 2.8. It was reported that most of ONOOH would be decomposed into NO_3^- and H^+ (Equation (13)) [16]. Thus, we speculated that peroxynitrite was decomposed via this reaction. The increase in NO_3^- during the extension of storage time could also verify this viewpoint (Figure 3e). The slight increase of electrical conductivity from 400 to 480 $\mu\text{S}/\text{cm}$ during 24-h storage may be attributed to the generation

of NO_3^- (Figure 3c). While there was no significant change in ORP with the increasing storage time. This may be attributed to the pH, which was an important factor influencing ORP [32].



3.3. The Inactivation of *A. flavus* by PAW

Although the fungicidal ability of PAW has been evidenced [18,33], the influence of storage time on the fungicidal efficiency of PAW was rarely studied. As was shown in Figure 4, the instant-prepared PAW exhibited the best fungicidal ability, which achieved a 3.22 Log reduction of *A. flavus* after 60-min treatment. When the PAW was stored at different times, its fungicidal ability was reduced quickly. A 60-min PAW treatment could only reduce 0.7 Log of *A. flavus* after 1-h storage. When the storage time reached 4 h, the fungicidal ability of PAW almost disappeared, which was the same as that of water treatment (Figure 4). According to the detection of peroxyntirite in PAW (Figure 3d), the fungicidal ability of PAW was consistent with the change of peroxyntirite, which indicated that peroxyntirite plays an important role in *A. flavus* inactivation by PAW.

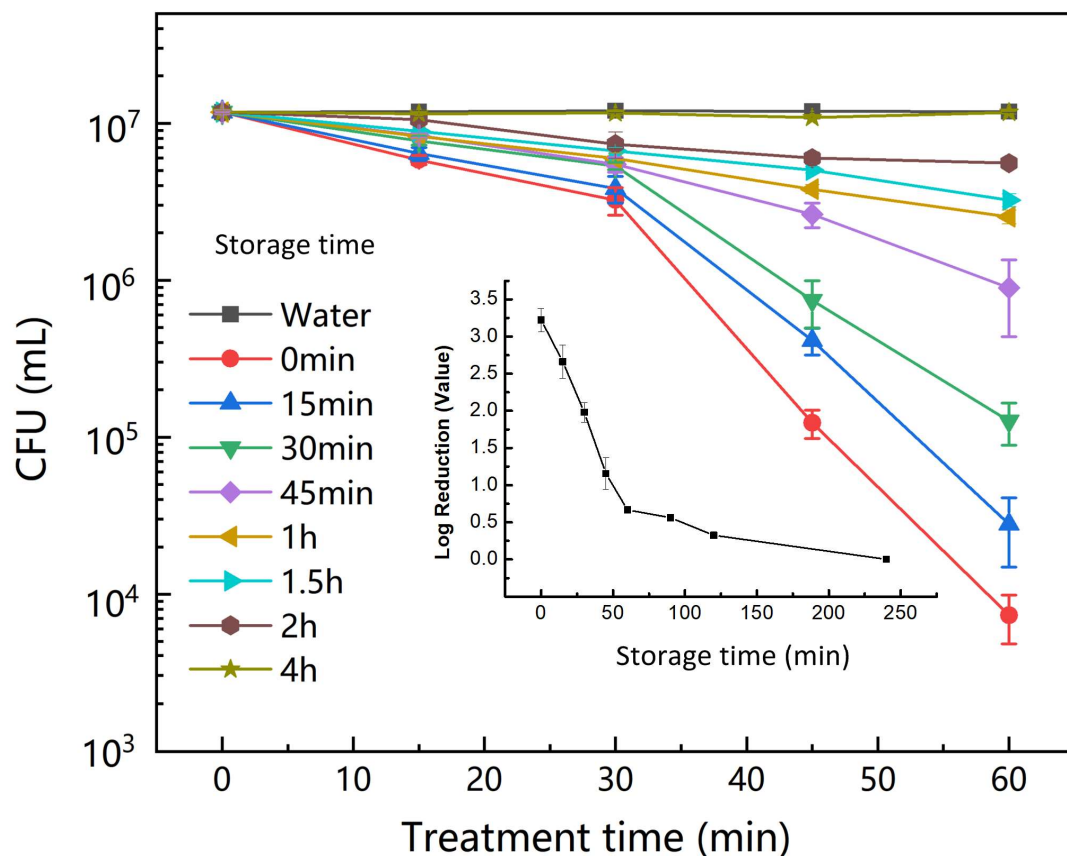


Figure 4. The changes of CFU treated by PAW at different storage times.

3.4. The Antifungal Mechanism of *A. flavus* by PAW

It was reported that RONS in PAW could induce membrane oxidative damage [18]. Among RONS, peroxyxynitrite could lead to lipid peroxidation and nitration [16]. Under the condition of low pH, peroxyxynitrite mainly in the form of ONOOH could cross the lipid bilayer in the cell membrane, and then initiate membrane peroxidation [34]. As was shown in Figure 5a, the cell membrane integrity of *A. flavus* spores was damaged. The enhancement of the permeability will contribute to the penetration of RONS into the cell, which can damage the cellular components and lead to the death of *A. flavus*. As was shown in Figure 5b,c, with the increase in PAW treatment time, both intracellular ONOO⁻ and NO increased. Differently, after 15 min PAW treatment, the increase in NO was more obvious than ONOO⁻. The reason may be that ONOO⁻ was not easy to enter a cell when the membrane was relatively intact. While, NO was more stable and highly diffusible, which could enter the cells easily [34]. Mitochondria dysfunction is an important intracellular event for the fungal inactivation induced by CAP or PAW [18,35]. As was shown in Figure 5d, PAW induced the depolarization of MMP. NO could lead to the loss of MMP through signal regulation (glutamate-receptor activation) [36]. In addition, NO could regulate ATP synthesis by inhibiting cytochrome c oxidase [37]. ONOO⁻ could inactivate the complex I, II, and V, as well as the electron transport-related enzymes, thus inducing mitochondrial dysfunction [19]. Thus, the increase in NO and ONOO⁻ could lead to a drop in MMP, which resulted in the death of *A. flavus* eventually.

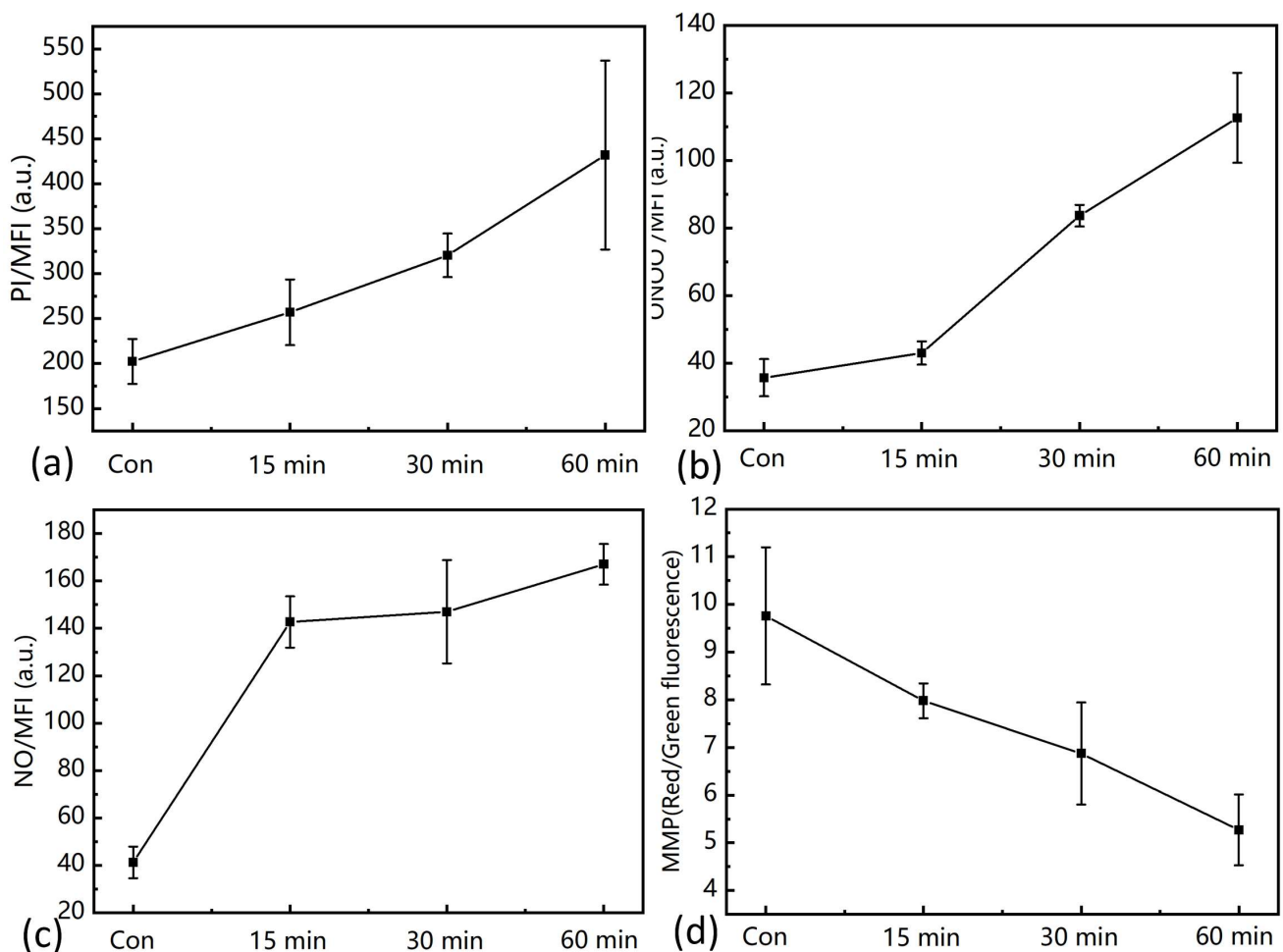


Figure 5. The change of (a) cell membrane integrity, (b) intracellular ONOO⁻, (c) NO, and (d) mitochondrial membrane potential after PAW treatment for 15, 30, and 60 min.

In addition to *A. flavus* spores, the change in cell membrane integrity, intracellular ONOO^- and NO, and MMP in *A. flavus* mycelium was also detected. As was shown in Figure 6, PAW treatment could also lead to the increase in cell membrane permeability and intracellular NO and ONOO^- , as well as the depolarization of MMP. These results indicated that PAW could also inactivate *A. flavus* mycelium.

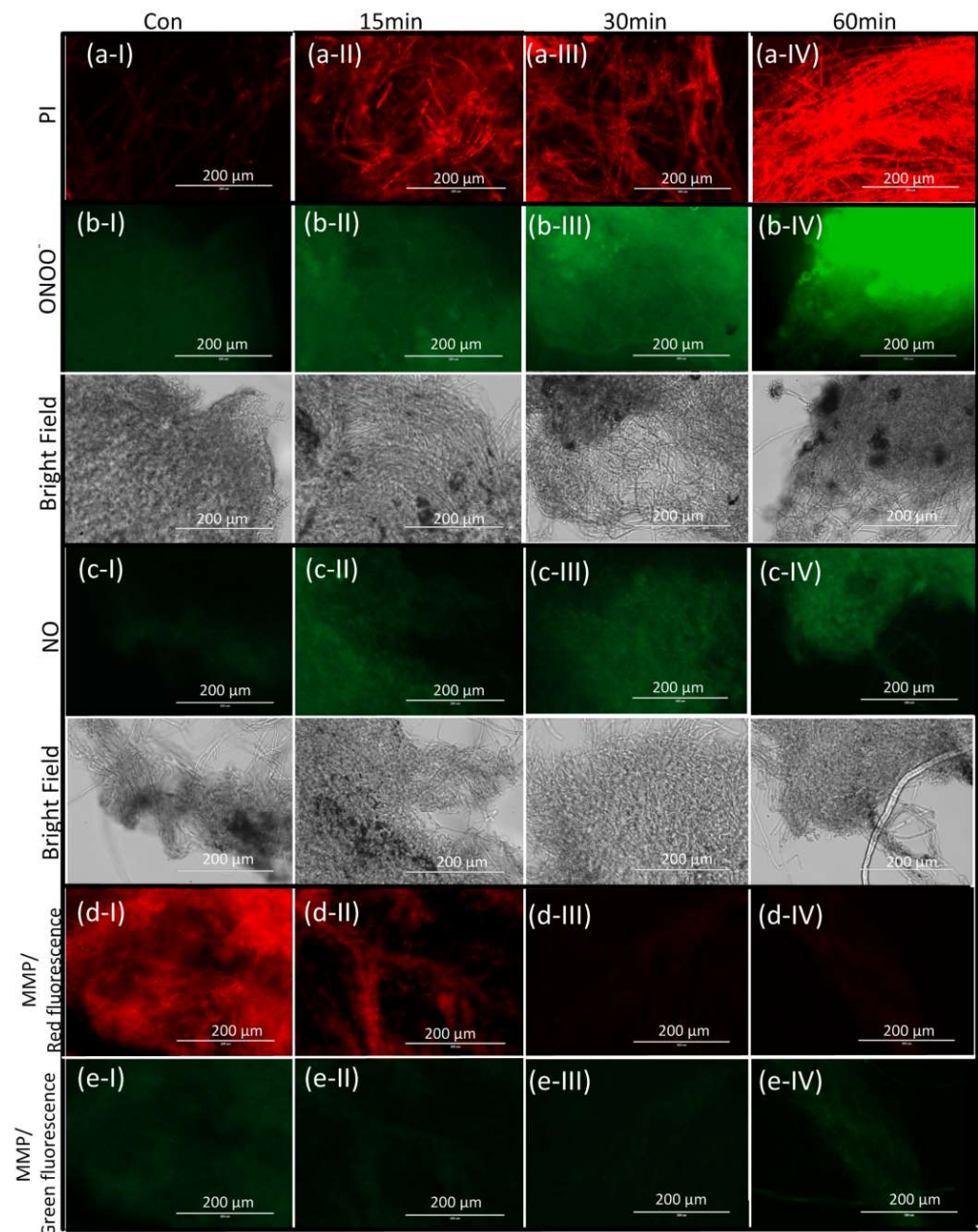


Figure 6. The change of (a) cell membrane integrity, (b) intracellular ONOO^- , (c) NO, and (d,e) mitochondrial membrane potential in *A. flavus* mycelium after PAW treatment for 15, 30 and 60 min.

3.5. The Inhibition of AFB_1 Synthesis by PAW

Besides the fungicidal ability of PAW, the long-term influence of PAW on fungal growth and AFB_1 synthesis in *A. flavus* was also investigated. After the instant-prepared PAW treatment, the spores were inoculated onto PDA and cultivated for 2, 3, and 5 d. As was shown in Figure 7, the content of AFB_1 reached 120 ppm after 5-d cultivation in the control group, while the content of AFB_1 in the PAW treatment group was about 14 ppm.

The result indicated that PAW treatment could influence the AFB₁ synthesis of *A. flavus*. The influence of plasma treatment on intracellular redox homeostasis and energy metabolism was considered the key reason for inducing fungal biological effects [35]. Therefore, we investigated the change of intracellular ATP, SOD, and CAT activity during 5-d cultivation after PAW treatment. It was found that ATP in the PAW treatment group was less than that in the control group. While SOD and CAT activity were higher compared with the control group (Figure 7). Liao et al. reported that the oxidative stress response triggered by plasma treatment will consume more cellular energy [38]. Thus, the energy assigned for other physiological activities might be reduced. It was speculated that the energy assigned for AFB₁ synthesis might be reduced when *A. flavus* suffered the oxidative stress of PAW treatment, thus leading to the decrease in AFB₁. In addition, it was reported that plasma treatment could disrupt mitochondrial function and decrease acetyl-CoA contents [39]. Acetyl-CoA is the precursor of Aflatoxins (AFs), which can be cyclized by the polyketide synthase. With a series of enzymatic reactions, AFs can be synthesized [40]. PAW treatment might disrupt the mitochondrial function and decrease acetyl-CoA contents, thus inhibiting the synthesis of AFB₁. Meanwhile, the enhancement of antioxidant enzymatic activities might inhibit AFB₁ synthesis. For example, dithiothreitol, and dimethyl sulfoxide can inhibit AFB₁ synthesis with an increase in SOD enzymatic activity [41,42]. Similarly, it was reported that ascorbic acid, cinnamaldehyde, and piperine-induced AFB₁ decrease with an increase in CAT activity [42–44]. Therefore, the improvement of SOD and CAT activities might inhibit AFB₁ synthesis under PAW treatment.

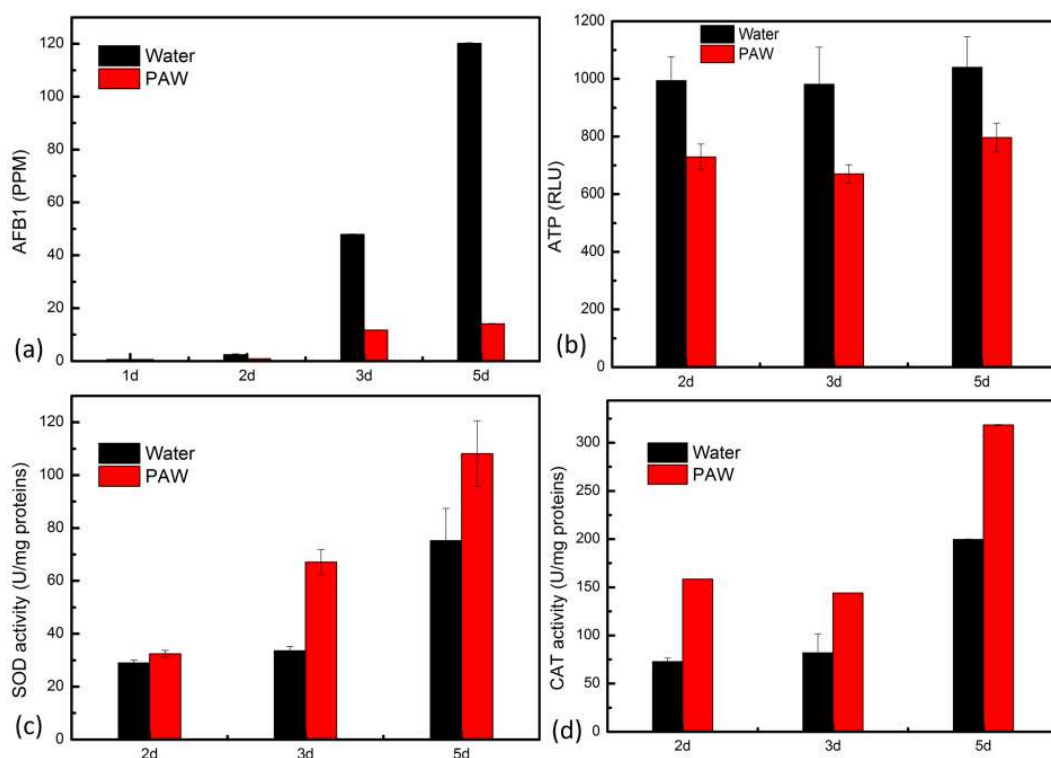


Figure 7. The changes of (a) AFB₁, (b) ATP, (c) SOD activity, and (d) CAT activity during 5-d cultivation before and after PAW treatment.

3.6. Inhibition of Key Genes Expression of AFB₁ Synthesis in *A. flavus* by PAW

In *A. flavus*, the biosynthesis pathways of AFB₁ are organized by diverse regulatory and structural genes. About 25 genes residing in a 75 kb cluster can encode more than 18 enzymes [45]. The structural genes of *aflD*, *AflP*, and *aflQ* encode three kinds of key enzymes in the biosynthesis pathways of AFB₁. *AflD*-encoded enzyme is responsible for the conversion of norsolorinic acid (NOR) to averantin (AVN). *AflP*-encoded enzymes are necessary for converting sterigmatocystin (ST) to o-methylsterigmatocystin (OMST). And

aflQ-encoded enzymes are necessary for converting OMST to AFB₁. The relative expression of these three structural genes was examined. As was shown in Figure 8, all of these three genes were downregulated during 5d cultivation. *aflR* and *aflS* are key regulatory genes in the synthesis of AFB₁ [26]. We also examined the relative expression of these two genes. As was shown in Figure 8, the expression of these two genes was also downregulated during 5-d cultivation. It was speculated that the changes in intracellular redox homeostasis and energy metabolism induced by PAW could regulate the expression of genes involved in the AFB₁ synthesis pathway, consequently decreasing AFB₁ biosynthesis in *A. flavus*.

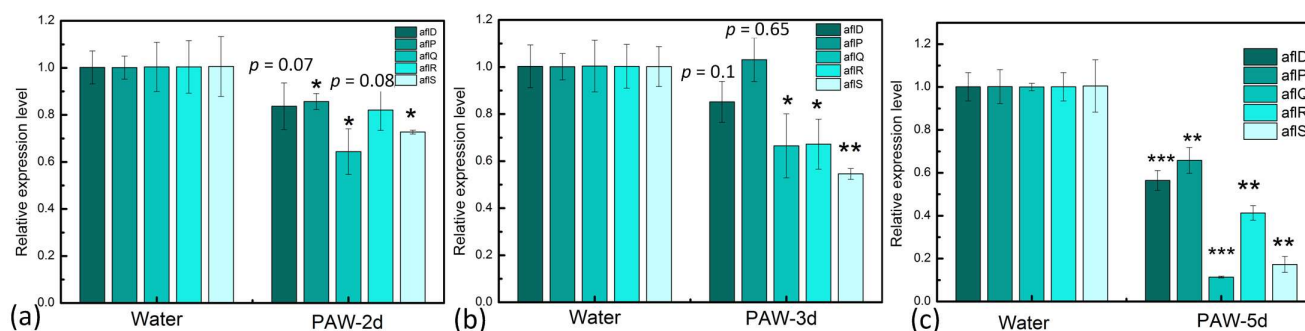


Figure 8. The relative expression levels of *aflD*, *aflP*, *aflQ*, *aflR* and *aflS* genes involved in the synthesis of AFB₁ during 2-d (a), 3-d (b) and 5-d (c) cultivation before and after PAW treatment. Significantly different values are expressed as * $p < 0.05$, ** $p < 0.01$, *** $p < 0.0001$.

4. Conclusions

In this study, the immediate fungicidal effect and long-term inhibitory effect of PAW on *A. flavus* were investigated. PAW could efficiently inactivate *A. flavus*, which was attributed to the increase in cell membrane permeability and intracellular NO and ONOO[−] as well as the depolarization of mitochondrial membrane potential. The fungicidal ability of PAW almost disappeared after 4-h storage. Besides the immediate fungicidal effect, PAW also exhibited long-term fungistatic properties. PAW treatment could inhibit AFB₁ production by inhibiting the expression of key genes involved in AFB₁ biosynthesis. Peroxynitrite was considered to play a critical role in the inactivation and inhibition of *A. flavus*. This study could provide new guidance for the application of low-temperature plasma technology especially PAW in the fungal and mycotoxin decontamination.

Supplementary Materials: The following supporting information can be downloaded at: <https://www.mdpi.com/article/10.3390/foods12132490/s1>, Table S1: The list of primers and the corresponding clustered aflatoxin biosynthesis pathway genes showing enzymes involved and their functions in the study; Figure S1: Representative standard curves and efficiency of each pair of primers. (a) β -Tubulin, (b) *aflD*, (c) *aflP*, (d) *aflQ*, (e) *aflR*, and (f) *aflS*. (Solid red lines denote the theoretical calculation curves. Dashed black lines indicate measurement curves).

Author Contributions: Conceptualization, D.C. and R.M.; software, Q.Y.; validation, H.X.; formal analysis, Q.Y. and H.X.; investigation, Q.Y. and H.X.; data curation, Q.Y. and H.X.; writing—original draft preparation, Q.Y. and H.X.; writing—review and editing, J.Z., D.C., R.M. and Z.J.; supervision, D.C. and R.M.; project administration, R.M.; funding acquisition, R.M. All authors have read and agreed to the published version of the manuscript.

Funding: This research was funded by the National Natural Science Foundation of China (11605159, 32101530, and 82200758), the Chinese Postdoctoral Science Foundation (2017M612412), the Foundation of Key Technology Research Project of Henan Province (222102110075 and 222102110031), the Open Project of State Key Laboratory of Cotton Biology (CB2022A12 and CB2022A15), the Young Talent and Enterprise Cooperative Innovation Team Support Project of Zhengzhou University (151/32320454), the Key Discipline Construction Project of Zhengzhou University (32410257), the Natural Science Foundation of Henan (222300420282), the Youth Innovation Project of Key Discipline of Zhengzhou University (XKZDQN202002), Scientific Research and Innovation Team of the First Af-

filiated Hospital of Zhengzhou University (QNCXTD2023005), and Guangzhou Medical Key Subject Construction Project (2021–2023).

Data Availability Statement: Data will be made available on request.

Conflicts of Interest: The authors declare no conflict of interest.

References

1. Misra, N.N.; Yadav, B.; Roopesh, M.S.; Jo, C. Cold Plasma for Effective Fungal and Mycotoxin Control in Foods: Mechanisms, Inactivation Effects, and Applications. *Compr. Rev. Food Sci. Food Saf.* **2019**, *18*, 106–120. [[CrossRef](#)] [[PubMed](#)]
2. Ott, L.C.; Appleton, H.J.; Shi, H.; Keener, K.; Mellata, M. High voltage atmospheric cold plasma treatment inactivates *Aspergillus flavus* spores and deoxynivalenol toxin. *Food Microbiol.* **2021**, *95*, 103669. [[CrossRef](#)] [[PubMed](#)]
3. Lin, C.M.; Patel, A.K.; Chiu, Y.C.; Hou, C.Y.; Kuo, C.H.; Dong, C.D.; Chen, H.L. The application of novel rotary plasma jets to inhibit the aflatoxin-producing *Aspergillus flavus* and the spoilage fungus, *Aspergillus niger* on peanuts. *Innov. Food Sci. Emerg. Technol.* **2022**, *78*, 102994. [[CrossRef](#)]
4. Xiong, K.; Liu, H.J.; Li, L.T. Product Identification and Safety Evaluation of Aflatoxin B₁ Decontaminated by Electrolyzed Oxidizing Water. *J. Agric. Food Chem.* **2012**, *60*, 9770–9778. [[CrossRef](#)] [[PubMed](#)]
5. López, M.; Calvo, T.; Prieto, M.; Múgica-Vidal, R.; Muro-Fraguas, I.; Alba-Elías, F.; Alvarez-Ordóñez, A. A review on non-thermal atmospheric plasma for food preservation: Mode of action, determinants of effectiveness, and applications. *Front. Microbiol.* **2019**, *10*, 622. [[CrossRef](#)] [[PubMed](#)]
6. Hojnik, N.; Modic, M.; Ni, Y.; Filipič, G.; Cvelbar, U.; Walsh, J.L. Effective Fungal Spore Inactivation with an Environmentally Friendly Approach Based on Atmospheric Pressure Air Plasma. *Environ. Sci. Technol.* **2019**, *53*, 1893–1904. [[CrossRef](#)]
7. Shen, J.; Zhang, H.; Xu, Z.; Zhang, Z.; Cheng, C.; Ni, G.; Lan, Y.; Meng, Y.; Xia, W.; Chu, P.K. Preferential production of reactive species and bactericidal efficacy of gas-liquid plasma discharge. *Chem. Eng. J.* **2019**, *362*, 402–412. [[CrossRef](#)]
8. Dasan, B.G.; Boyaci, I.H.; Mutlu, M. Inactivation of aflatoxigenic fungi (*Aspergillus* spp.) on granular food model, maize, in an atmospheric pressure fluidized bed plasma system. *Food Control.* **2016**, *70*, 1–8. [[CrossRef](#)]
9. Dasan, B.G.; Mutlu, M.; Boyaci, I.H. Decontamination of *Aspergillus flavus* and *Aspergillus parasiticus* spores on hazelnuts via atmospheric pressure fluidized bed plasma reactor. *Int. J. Food Microbiol.* **2016**, *216*, 50–59. [[CrossRef](#)]
10. Dasan, B.G.; Boyaci, I.H.; Mutlu, M. Nonthermal plasma treatment of *Aspergillus* spp. spores on hazelnuts in an atmospheric pressure fluidized bed plasma system: Impact of process parameters and surveillance of the residual viability of spores. *J. Food Eng.* **2017**, *196*, 139–149. [[CrossRef](#)]
11. Devi, Y.; Thirumdas, R.; Sarangapani, C.; Deshmukh, R.R.; Annapure, U.S. Influence of cold plasma on fungal growth and aflatoxins production on groundnuts. *Food Control.* **2017**, *77*, 187–191. [[CrossRef](#)]
12. Mošovská, S.; Medvecká, V.; Gregová, M.; Tomeková, J.; Valík, L.; Mikulajová, A.; Zahoranová, A. Plasma inactivation of *Aspergillus flavus* on hazelnut surface in a diffuse barrier discharge using different working gases. *Food Control* **2019**, *104*, 256–261. [[CrossRef](#)]
13. Herianto, S.; Hou, C.Y.; Lin, C.M.; Chen, H.L. Nonthermal plasma-activated water: A comprehensive review of this new tool for enhanced food safety and quality. *Compr. Rev. Food Sci. Food Saf.* **2021**, *20*, 583–626. [[CrossRef](#)]
14. Zheng, Y.; Wu, S.; Dang, J.; Wang, S.; Liu, Z.; Fang, J.; Han, P.; Zhang, J. Reduction of phoxim pesticide residues from grapes by atmospheric pressure non-thermal air plasma activated water. *J. Hazard. Mater.* **2019**, *377*, 98–105. [[CrossRef](#)]
15. Cooper, M.; Fridman, G.; Fridman, A.; Joshi, S. Biological responses of *Bacillus stratosphericus* to Floating Electrode-Dielectric Barrier Discharge Plasma Treatment. *J. Appl. Microbiol.* **2010**, *109*, 2039–2048. [[CrossRef](#)]
16. Zhou, R.; Zhou, R.; Prasad, K.; Fang, Z.; Speight, R.; Bazaka, K.; Ostrikov, K. Cold atmospheric plasma activated water as a prospective disinfectant: The crucial role of peroxydinitrite. *Green Chem.* **2018**, *20*, 5276–5284. [[CrossRef](#)]
17. Zhou, R.; Zhou, R.; Wang, P.; Xian, Y.; Mai-Prochnow, A.; Lu, X.P.; Cullen, P.J.; Ostrikov, K.; Bazaka, K. Plasma-activated water: Generation, origin of reactive species and biological applications. *J. Phys. D Appl. Phys.* **2020**, *53*, 303001. [[CrossRef](#)]
18. Guo, J.; Wang, J.; Xie, H.; Jiang, J.; Li, C.; Li, W.; Li, L.; Liu, X.; Lin, F. Inactivation effects of plasma-activated water on *Fusarium graminearum*. *Food Control* **2022**, *134*, 108683. [[CrossRef](#)]
19. Guo, L.; Yao, Z.; Yang, L.; Zhang, H.; Qi, Y.; Gou, L.; Xi, W.; Liu, D.; Zhang, L.; Cheng, Y.; et al. Plasma-activated water: An alternative disinfectant for S protein inactivation to prevent SARS-CoV-2 infection. *Chem. Eng. J.* **2021**, *421*, 127742. [[CrossRef](#)]
20. Ma, R.; Wang, G.; Tian, Y.; Wang, K.; Zhang, J.; Fang, J. Non-thermal plasma-activated water inactivation of food-borne pathogen on fresh produce. *J. Hazard. Mater.* **2015**, *300*, 643–651. [[CrossRef](#)]
21. Lukes, P.; Dolezalova, E.; Sisrova, I.; Clupek, M. Aqueous-phase chemistry and bactericidal effects from an air discharge plasma in contact with water: Evidence for the formation of peroxydinitrite through a pseudo-second-order post-discharge reaction of H₂O₂ and HNO₂. *Plasma Sources Sci. Technol.* **2014**, *23*, 5019. [[CrossRef](#)]
22. Balazinski, M.; Schmidt-Bleker, A.; Winter, J.; von Woedtke, T. Peroxydinitrous Acid Generated In Situ from Acidified H₂O₂ and NaNO₂. A Suitable Novel Antimicrobial Agent? *Antibiotics* **2021**, *10*, 1003. [[CrossRef](#)] [[PubMed](#)]
23. Herianto, S.; Arcega, R.D.; Hou, C.Y.; Chao, H.R.; Lee, C.C.; Lin, C.M.; Mahmudiono, T.; Chen, H.L. Chemical decontamination of foods using non-thermal plasma-activated water. *Sci. Total Environ.* **2023**, *874*, 162235. [[CrossRef](#)] [[PubMed](#)]

24. Tarabová, B.; Lukeš, P.; Hammer, M.U.; Jablonowski, H.; von Woedtke, T.; Reuter, S.; Machala, Z. Fluorescence measurements of peroxyxynitrite/peroxyxynitrous acid in cold air plasma treated aqueous solutions. *Phys. Chem. Chem. Phys.* **2019**, *21*, 8883–8896. [[CrossRef](#)] [[PubMed](#)]
25. Tian, Y.; Ma, R.; Zhang, Q.; Feng, H.; Liang, Y.; Zhang, J.; Fang, J. Assessment of the Physicochemical Properties and Biological Effects of Water Activated by Non-thermal Plasma Above and Beneath the Water Surface. *Plasma Process. Polym.* **2015**, *12*, 439–449. [[CrossRef](#)]
26. Youssef, N.H.; Qari, S.H.; Matar, S.; Hamad, N.A.; Dessoky, E.S.; Elshaer, M.M.; Sobhy, S.; Abdelkhalik, A.; Zakaria, H.M.; Heflish, A.A.; et al. Licorice, Doum, and Banana Peel Extracts Inhibit *Aspergillus flavus* Growth and Suppress Metabolic Pathway of Aflatoxin B1 Production. *Agronomy* **2021**, *11*, 1587. [[CrossRef](#)]
27. Livak, K.J.; Schmittgen, T.D. Analysis of relative gene expression data using real-time quantitative PCR and the 2[−]ΔΔCT method. *Methods* **2001**, *25*, 402–408. [[CrossRef](#)]
28. Xu, H.; Zhu, Y.; Cui, D.; Du, M.; Wang, J.; Ma, R.; Jiao, Z. Evaluating the roles of OH radicals, H₂O₂, ORP and pH in the inactivation of yeast cells on a tissue model by surface micro-discharge plasma. *J. Phys. D Appl. Phys.* **2019**, *52*, 395201. [[CrossRef](#)]
29. Kim, S.J.; Joh, H.M.; Chung, T.H. Production of intracellular reactive oxygen species and change of cell viability induced by atmospheric pressure plasma in normal and cancer cells. *Appl. Phys. Lett.* **2013**, *103*, 153705. [[CrossRef](#)]
30. Wang, Z.; Qi, Y.; Guo, L.; Huang, L.; Yao, Z.; Yang, L.; Li, G.; Chen, J.; Yan, J.; Niyazi, G.; et al. The bactericidal effects of plasma-activated saline prepared by the combination of surface discharge plasma and plasma jet. *J. Phys. D Appl. Phys.* **2021**, *54*, 385202. [[CrossRef](#)]
31. Wang, W.; Guo, L.; Yao, Z.; Xi, W.; Zhao, Y.; Lv, J.; Zhang, J.; Liu, Z.; Liu, D. Nitrox surface discharge used for water activation: The reactive species and their correlation to the bactericidal effect. *J. Phys. D Appl. Phys.* **2022**, *55*, 265203. [[CrossRef](#)]
32. Van Haute, S.; Zhou, B.; Luo, Y.; Sampers, I.; Vanhaverbeke, M.; Millner, P. The use of redox potential to estimate free chlorine in fresh produce washing operations: Possibilities and limitations. *Postharvest Biol. Technol.* **2019**, *156*, 110957. [[CrossRef](#)]
33. Los, A.; Ziuzina, D.; Boehm, D.; Cullen, P.J.; Bourke, P. Inactivation Efficacies and Mechanisms of Gas Plasma and Plasma-Activated Water against *Aspergillus flavus* Spores and Biofilms: A Comparative Study. *Appl. Environ. Microbiol.* **2020**, *86*, e02619-19. [[CrossRef](#)]
34. Szabó, C.; Ischiropoulos, H.; Radi, R. Peroxynitrite: Biochemistry, pathophysiology and development of therapeutics. *Nat. Rev. Drug Discov.* **2007**, *6*, 662–680. [[CrossRef](#)]
35. Xu, H.; Zhu, Y.; Du, M.; Wang, Y.; Ju, S.; Ma, R.; Jiao, Z. Subcellular mechanism of microbial inactivation during water disinfection by cold atmospheric-pressure plasma. *Water Res.* **2021**, *188*, 116513. [[CrossRef](#)]
36. Moncada, S.; Bolanos, J.P. Nitric oxide, cell bioenergetics and neurodegeneration. *J. Neurochem.* **2006**, *97*, 1676–1689. [[CrossRef](#)]
37. Beltrán, B.; Mathur, A.; Duchon, M.R.; Erusalimsky, J.D.; Moncada, S. The effect of nitric oxide on cell respiration: A key to understanding its role in cell survival or death. *Proc. Natl. Acad. Sci. USA* **2000**, *97*, 14602–14607. [[CrossRef](#)]
38. Liao, X.; Liu, D.; Ding, T. Nonthermal Plasma Induces the Viable-but-Nonculturable State in *Staphylococcus aureus* via Metabolic Suppression and the Oxidative Stress Response. *Appl. Environ. Microbiol.* **2020**, *86*, e02216-19. [[CrossRef](#)]
39. Wang, Y.; Li, B.; Shang, H.; Ma, R.; Zhu, Y.; Yang, X.; Ju, S.; Zhao, W.; Sun, H.; Zhuang, J.; et al. Effective inhibition of fungal growth, deoxynivalenol biosynthesis and pathogenicity in cereal pathogen *Fusarium* spp. by cold atmospheric plasma. *Chem. Eng. J.* **2022**, *437*, 135307. [[CrossRef](#)]
40. Li, X.; Jiang, Y.; Ma, L.; Ma, X.; Liu, Y.; Shan, J.; Ma, K.; Xing, F. Comprehensive Transcriptome and Proteome Analyses Reveal the Modulation of Aflatoxin Production by *Aspergillus flavus* on Different Crop Substrates. *Front. Microbiol.* **2020**, *11*, 1497. [[CrossRef](#)]
41. Reverberi, M.; Fabbri, A.A.; Zjalic, S.; Ricelli, A.; Punelli, F.; Fanelli, C. Antioxidant enzymes stimulation in *Aspergillus parasiticus* by *Lentinula edodes* inhibits aflatoxin production. *Appl. Microbiol. Biotechnol.* **2005**, *69*, 207–215. [[CrossRef](#)] [[PubMed](#)]
42. Grintzalis, K.; Vernardis, S.I.; Klapa, M.I.; Georgiou, C.D. Role of Oxidative Stress in Sclerotial Differentiation and Aflatoxin B1 Biosynthesis in *Aspergillus flavus*. *Appl. Environ. Microbiol.* **2014**, *80*, 5561–5571. [[CrossRef](#)] [[PubMed](#)]
43. Caceres, I.; El Khoury, R.; Bailly, S.; Oswald, I.P.; Puel, O.; Bailly, J.D. Piperine inhibits aflatoxin B1 production in *Aspergillus flavus* by modulating fungal oxidative stress response. *Fungal Genet. Biol.* **2017**, *107*, 77–85. [[CrossRef](#)] [[PubMed](#)]
44. Sun, Q.; Shang, B.; Wang, L.; Lu, Z.; Liu, Y. Cinnamaldehyde inhibits fungal growth and aflatoxin B1 biosynthesis by modulating the oxidative stress response of *Aspergillus flavus*. *Appl. Microbiol. Biotechnol.* **2016**, *100*, 1355–1364. [[CrossRef](#)]
45. Cleveland, T.E.; Yu, J.; Fedorova, N.; Bhatnagar, D.; Payne, G.A.; Nierman, W.C.; Bennett, J.W. Potential of *Aspergillus flavus* genomics for applications in biotechnology. *Trends Biotechnol.* **2009**, *27*, 151–157. [[CrossRef](#)]

Disclaimer/Publisher’s Note: The statements, opinions and data contained in all publications are solely those of the individual author(s) and contributor(s) and not of MDPI and/or the editor(s). MDPI and/or the editor(s) disclaim responsibility for any injury to people or property resulting from any ideas, methods, instructions or products referred to in the content.